

January 6, 2008.

# The Cepheid Period-Luminosity Relation at Mid-Infrared Wavelengths: I. First-Epoch LMC Data

Wendy L. Freedman, Barry F. Madore, Jane Rigby, S. E. Persson

*Observatories of the Carnegie Institution of Washington  
813 Santa Barbara St., Pasadena, CA 91101*

wendy@ociw.edu, barry@ociw.edu, jrigby@ociw.edu, persson@ociw.edu

**& Laura Sturch**

*Harvey Mudd College  
Claremont CA 91711*

laura.sturch@hmc.edu

## ABSTRACT

We present the first mid-infrared Period-Luminosity (PL) relations for Large Magellanic Cloud (LMC) Cepheids. Single-epoch observations of 70 Cepheids were extracted from Spitzer IRAC observations at 3.6, 4.5, 5.8 and 8.0  $\mu\text{m}$ , serendipitously obtained during the SAGE (Surveying the Agents of a Galaxy's Evolution) imaging survey of the LMC. All four mid-infrared PL relations have nearly identical slopes over the period range 6 - 88 days, with a small scatter of only  $\pm 0.16$  mag independent of period for all four of these wavelengths. We emphasize that differential reddening is not contributing significantly to the observed scatter, given the nearly two orders of magnitude reduced sensitivity of the mid-IR to extinction compared to the optical. Future observations, filling in the light curves for these Cepheids, should noticeably reduce the residual scatter. These attributes alone suggest that mid-infrared PL relations will provide a practical means of significantly improving the accuracy of Cepheid distances to nearby galaxies.

*Subject headings:* Cepheids — cosmology: distance scale — infrared: stars — Magellanic Clouds

## 1. INTRODUCTION

Distance measurements to the Large Magellanic Cloud (LMC) have historically played a critical role in the calibration of the extragalactic distance scale (Feast & Walker 1987; Madore & Freedman 1991; Udalski *et al.* 1999; Freedman *et al.* 2001; Sandage *et al.* 2006). The LMC Cepheid Period-Luminosity relations have been adopted as the fiducial calibration sample for many recent extragalactic distance measurements and for the determination of the Hubble constant (*e.g.*, Freedman *et al.* 2001, Sandage *et al.* 2006, Riess *et al.* 2005).

A number of different methods have been used to measure the distance to the LMC. As tabulated in Gibson (2000) and Freedman *et al.* (2001), most of the values for the LMC distance modulus based on these different methods fall between 18.1 to 18.7 mag, corresponding to a full range of 42 to 55 kpc, and likely reflecting the effects of systematic errors in various methods. More recent values have tended to cluster around a modulus of 18.5 mag (see Alves 2004; and also an interesting commentary by Schaefer 2007)<sup>1</sup>.

In an effort to reduce the systematic errors in the LMC distance, Persson *et al.* (2004) obtained near-infrared J, H, and K<sub>s</sub> photometric measurements of 92 LMC Cepheids. These stars were chosen to be distributed across the LMC, with periods ranging from 3 to 100 days. They were also selected to be relatively isolated so that crowding effects would be minimized. The sample also does not contain overtone pulsators. On average, 22 phase points were obtained at each wavelength for each star. The dispersions in the infrared PL, PLC, and extinction-free period-Wesenheit relations were found to be very small, amounting to less than  $\pm 0.14$  mag, or 7% in distance.

There are a number of advantages to obtaining observations of Cepheids at long wavelengths (see, for example, the reviews by Madore & Freedman (1991, 1998) and references therein): (1) The sensitivity of surface brightness to temperature is a steeply declining function of wavelength. (2) The interstellar extinction curve decreases as a function of increasing wavelength (being almost linear with  $1/\lambda$  at optical and near-infrared wavelengths). (3) At the temperatures typical of Cepheids, metallicity effects predominate in the UV, blue and visual parts of the spectrum where most of the line transitions occur, with declining effects at longer wavelengths (Bono *et al.* 1999). The overall insensitivity of infrared magnitudes of Cepheids to each of these effects results in decreased amplitudes for individual Cepheids, as well as a decreased scatter in the apparent PL relations (first noted by Wisniewski & Johnson 1968, and by McGonegal *et al.* 1982, respectively).

---

<sup>1</sup>For a regularly updated compilation of published distances to the Large Magellanic Cloud see the web site maintained by Ian Steer and Barry Madore through NED at [http://nedwww.ipac.caltech.edu/level5/NED0D/LMC\\_ref.html](http://nedwww.ipac.caltech.edu/level5/NED0D/LMC_ref.html).

Given the pivotal role of the LMC distance in calibrating the extragalactic distance scale, developing techniques to further reduce systematic errors in that path remains a critical goal. The mid-infrared capability of Spitzer offers a new opportunity to provide a distance modulus to the LMC completely freed from the effects of reddening and with decreased sensitivity to metallicity. As we discuss below, beyond about  $4.5 \mu\text{m}$ , the resulting extinction is at least a factor of 25 times smaller than the corresponding extinction in the B band.

We report here on single-epoch, mid-infrared data for a subset of the Persson *et al.* (2004) LMC sample, which were observed with Spitzer at 3.6, 4.5, 5.8 and  $8.0 \mu\text{m}$ . Data for 70 of the 92 Persson *et al.* Cepheids were serendipitously obtained in the course of the SAGE project (Meixner *et al.* 2006a), a large-area study of the interstellar medium and current star formation in the LMC. Since Cepheids are relatively young stars, large numbers of Cepheids were also observed in these fields, and fortunately, as we show here, they were observed with sufficient signal-to-noise to be suitable for our purposes also. The single-epoch, mid-IR Cepheid PL relations resulting from these observations have a total scatter of only  $\pm 0.16$  mag (8% in distance) for a single Cepheid with less than 1% (statistical) uncertainty in the mean for this sample. We discuss the prospects for reducing the scatter even further.

## 2. IRAC Mid-Infrared Period-Luminosity Relations

SAGE, the Spitzer survey of the Large Magellanic Cloud is an acronym for *Surveying the Agents of a Galaxy's Evolution* (Meixner *et al.* 2006a). The survey covers a  $7 \times 7$  degree region of the LMC using both the IRAC and MIPS detectors, operating at 3.6, 4.5, 5.8,  $8.0 \mu\text{m}$ , and 24, 70,  $160 \mu\text{m}$ , respectively. The MIPS far-infrared data were obtained to probe the diffuse dust emission in the LMC, while the IRAC data were obtained primarily to study the stellar content; in the context of this study, we have analyzed only the IRAC data. Two epochs of data have been obtained; however, at the time of writing SAGE had released catalogs based on the first epoch data only.

Catalogs of resolved sources have been prepared by the SAGE project and made available through the Infrared Science Archive (IRSA). We used the interface, GATOR, to retrieve the individual data files manually by object name based on a position-based cone search using the NED name resolver. Our in-going list of objects consisted of the 92 Cepheids with extensive JHK<sub>s</sub> photometry published by Persson *et al.* (2004). Only those Cepheids found in the catalog with periods between  $0.8 < \log(P[\text{days}]) < 1.8$  and having photometry at all four wavelengths were retained. This sample of 70 Cepheids is listed in Table 1, with the logarithm of the period in days (from Persson *et al.*), plus magnitudes and errors in each mid-infrared bandpass. The photometry is from Meixner *et al.* (2006a) and was obtained

using PSF fitting with a modified version of DAOPHOT, using an iterative technique to measure the local background. Magnitudes are on the Vega system.

The four mid-IR period-luminosity relations, based on single-epoch observations ranging from 3.6 to 8.0  $\mu\text{m}$ , are shown in Figures 1 and 2. SAGE mapped with half-array offsets, so that each epoch contains two 12-second integrations and thus the total IRAC integrations were 24 seconds for each epoch. For 139 calibration stars, the SAGE team compared their catalog magnitudes to those predicted from 2MASS fluxes (Meixner *et al.* 2006a). The systematic offsets are  $\sim 0.01$  mag, and the standard deviation is  $\sim 0.05$  mag in all four IRAC channels (Meixner *et al.* 2006b). Since the fainter calibrators have fluxes typical of our brighter Cepheids,  $\pm 0.05$  mag is a reasonable expectation for the typical  $1\text{-}\sigma$  uncertainty for our Cepheid photometry. This expectation is consistent with the quoted SAGE photometric uncertainties for our Cepheid sample, listed in Table 1.

As can be seen from Figures 1 and 2, the mid-infrared Period-Luminosity relations: (1) all show small scatter, which is similar in magnitude from filter to filter, (2) all four relations have very similar slopes, and (3) as can be seen from Figure 3, the residuals around the fits are highly correlated (with approximately unit slope) from one PL relation to the next. We note that the first two of these statements do not apply to the visual and blue PL relations. But before turning to address why this is the case, we first quantify the above statements.

## 2.1. Period-Luminosity Fits

Weighted, least-squares, linear fits to each of the four mid-IR data sets are given in §3. The slopes, zero points, respective errors and *rms* scatter are shown for each bandpass. The slopes at each wavelength all have values of around -3.4, with a slight trend of the slopes increasing to longer wavelengths. The scatter around each of the fits is constant at  $\pm 0.16$  mag; and, from filter to filter the scatter of individual data points is highly correlated (see Figure 3 and discussion below).

According to Gieren, Moffett & Barnes (1999) the best current estimate of the slope of the Period-Radius relation, using radial velocity studies of Magellanic Cloud and Milky Way Cepheids is  $\log(R) = 0.680 \log(P) + C$ . If we convert  $\log(R)$  to an area and then express it as a magnitude, the slope derived from the Period-Radius relation  $(0.680 \pm 0.017) \times -5 = 3.40 \pm 0.085$  is statistically indistinguishible from the longest-wavelength mid-IR PL slopes of  $3.44 \pm 0.03$  and  $3.42 \pm 0.03$  at 8.0 and 5.8  $\mu\text{m}$ , respectively. This agreement suggests that the mid-IR PL relation is in fact the Period-Area relation at fixed surface brightness. All of these mid-IR wavelengths have small sensitivities to temperature, which may also explain

the similarity of slopes, as well as the small magnitude of the scatter.

In Figure 4 we show the run of PL slopes as a function of increasing wavelength, from the optical to the mid-infrared. The optical (BVRI) slopes are from Madore & Freedman (1998); near-infrared (JHK) slopes are from Persson et al. (2004); and mid-IR slopes are from the present paper. Following the dramatic change seen at optical wavelengths, the slope appears to be asymptotically approaching a value of about -3.45, which is within the currently published uncertainties for pure radius variations (i.e.  $3.40 \pm 0.085$ ). The latter is shown by the horizontal lines crossing the bottom of Figure 4.

## 2.2. Correlations in the Scatter

The correlated nature of the small residual scatter in the mid-IR can be explained by three contributors. For an intrinsically uniform distribution of data points (as is the case for a Cepheid light curve) the variance is formally equal to the range (i.e., the full amplitude) divided by 12. If the typical amplitude of a Cepheid in the mid-IR is comparable to the amplitudes seen in the near-IR, 0.4 mag say, then the equivalent scatter contributed to the observed PL relation due to random sampling of the light curve would be  $0.40/\sqrt{12} = \pm 0.11$  mag. If we remove (in quadrature) this random-phase induced scatter (0.11 mag) from the total measured scatter (0.16 mag) we are left with  $[(0.16)^2 - (0.11)^2]^{1/2} = 0.12$  mag, and we can simply draw the following conclusions: Half of the correlation is simply due to the random sampling of the (highly correlated) light curves, which at these wavelengths, have equal amplitudes and tightly matched phases. The other half of the scatter comes from the correlated nature of the mean-light position of an individual Cepheid within the parent instability strip: that is, at a given period brighter Cepheids are brighter at all wavelengths, either due to systematic temperature differences, radius differences, or both. In either case, the amplitude of this correlation is expected to be reduced in the mid-IR, but it is still predicted to be coupled wavelength to wavelength, as is indeed seen in these datasets.

Figure 3 also illustrates that the (second-order) scatter around the filter-filter residual plots (for example,  $\pm 0.057$  mag scatter about a regression line of slope  $+0.98 \pm 0.01$  in the 3.6 versus 5.8  $\mu\text{m}$  correlation) is consistent with the range of (individually plotted) observational errors of  $\pm 0.03$ - $0.09$  mag given for the SPITZER data in Table 1.

### 2.3. Reddening

From optical studies, estimated reddening values for these LMC Cepheids range from  $E(B-V) = 0.00$  to  $0.20$  mag (e.g., Martin, Warren & Feast 1979). The mid-IR extinction curve of the LMC has not been measured, but measurements of the Galactic extinction curve (Lutz et al. 1996; Indebetouw et al. 2005; Flaherty et al. 2007; Roman-Zuniga et al. 2007), when scaled from  $A_K$  to  $A_V$  via Rieke & Lebofsky (1985), find  $A_{5.8\mu m} / A_K = 0.4$  to  $0.5$ , and  $A_{5.8\mu m} / A_B \approx 0.04$ .

As an example, the most extreme value of  $E(B-V)$  given above,  $0.20$  mag, yields  $A_B = 4.2 \times E(B-V) = 0.84$  mag. This converts to  $A_{5.8\mu m} = 0.03$  mag, which is close to the photometric precision of the current dataset. Most LMC Cepheids have a typical reddening being perhaps a factor of two smaller (i.e.,  $E(B-V) = 0.10$  mag). Thus, *differential reddening effects* around a mean value of  $E(B-V) = 0.10$  mag would impact the intrinsic calibration of the mid-IR PL relations for LMC Cepheids at the level of only  $\pm 0.01$  mag. This is a huge advantage for measuring precise and accurate extragalactic distances.

## 3. Absolute Calibration

For the purposes of the present paper, we adopt a true distance to the Large Magellanic Cloud of  $(m-M)_o = 18.50$  mag and a mean reddening to the Cepheids of  $E(B-V) = 0.10$  mag (consistent with the values adopted by the HST Key Project, Freedman *et al.*, 2001). Applying this offset in true distance modulus, subtracting the small corrections for extinction ( $0.04$  to  $0.01$  mag), and using simple least-squares fitting we derive the following provisional absolute calibrations for the Cepheid Period-Luminosity relations at mid-infrared wavelengths:

$$M_{3.6} = -3.34(\log(P) - 1.0) [\pm 0.02] - 5.87 [\pm 0.02]$$

$$M_{4.5} = -3.29(\log(P) - 1.0) [\pm 0.03] - 5.92 [\pm 0.03]$$

$$M_{5.8} = -3.42(\log(P) - 1.0) [\pm 0.03] - 5.83 [\pm 0.02]$$

$$M_{8.0} = -3.44(\log(P) - 1.0) [\pm 0.03] - 5.89 [\pm 0.02]$$

These mid-infrared Period-Luminosity relations and their calibration hold much promise for improvement. The second-epoch SAGE data is expected to be released within the next year. Spitzer mid-IR observations of several nearby Galactic field Cepheids can also provide an independent *absolute* calibration for these PL relations, based on the geometric parallax distances determined recently by Benedict *et al.* (2007) using the Hubble Space Telescope Fine-Guidance Sensors. Furthermore, we hope to extend the observations for this sample to obtain multi-epoch, mid-infrared data (and time-averaged magnitudes and colors) during the upcoming final cycle for cold Spitzer observations. In the future, NIRCAM and MIRI on JWST will be able to provide mid-infrared PL relations for known Cepheids in nearby galaxies, and a re-calibration of the extragalactic distance scale.

#### 4. Conclusions

We have presented the first absolute calibrations of the Cepheid Period-Luminosity relations at four mid-infrared wavelengths. These relations are already good to  $\pm 0.02$  in the slope and  $\pm 0.04$  mag in their relative zero points. At each of these wavelengths the scatter is such that a single, random-phase observation of a single Cepheid can provide a distance that is good to  $\pm 8\%$  (statistical error alone). Given the mid-infrared imaging capabilities of JWST, we are optimistic that these calibrations can be used to determine high-precision distances to the most distant galaxies in which Cepheids have been so far discovered independent of most of the systematic effects that are currently limiting the accuracy of optical studies.

We thank the referee for constructive comments, and for suggesting the inclusion of Figure 4. This research has made use of the NASA/IPAC Extragalactic Database (NED) which is operated by the Jet Propulsion Laboratory, California Institute of Technology, under contract with the National Aeronautics and Space Administration.

*Facilities:* Spitzer

## References

- Alves, D. R., 2004, *New Astron.Rev.*, 48, 659
- Benedict, G. F., *et al.* 2007, *AJ*, 133, 1810
- Bono, G., Caputo, F., Castellani, V., & Marconi, M. 1999, *ApJ*, 512, 711
- Cardelli, J. A., Clayton, G. C., & Mathis, J. S. 1989, *ApJ*, 345, 245
- Feast, M. W., & Walker, A. R. 1987, *ARAA*, 25, 345
- Flaherty, K. M., Pipher, J. L., Megeath, S. T., Winston, E. M., Gutermuth, R. A., Muzerolle, J., Allen, L. E., & Fazio, G. G., 2007, *ApJ*, 663, 1069
- Freedman, W. L., *et al.* 2001, *ApJ*, 553, 47
- Gibson, B. K. 2000, *Memorie della Societa Astronomica Italiana*, 71, 693
- Gieren, W. P., Moffett, T. J., & Barnes, T. G. III. 1999, *ApJ*, 512, 553
- Indebetouw, R., *et al.*, 2005, *ApJ*, 619, 931
- Lutz, D., *et al.* 1996, *A&A*, 315, L269
- Madore, B. F., & Freedman, W. L. 1991, *PASP*, 103, 933
- Madore, B. F., & Freedman, W. L. 1998, “Stellar Astrophysics for the Local Group”, eds. A. Aparicio, A. Herrero & F. Sanchez, Cambridge University Press
- Martin, W. L., Warren, P. R., & Feast, M. J. 1979, *MNRAS*, 188, 139
- McGonegal, R., McAlary, C. W., Madore, B. F., & McLaren, R. A. 1982, *ApJ*, 257, L33
- Meixner, M., *et al.* 2006a, *AJ*, 132, 2268
- Meixner, M., *et al.* 2006b, “The SAGE Data Description: Delivery 1”  
[http://sage.stsci.edu/SAGE\\_SSCdatadocument\\_v5.pdf](http://sage.stsci.edu/SAGE_SSCdatadocument_v5.pdf)
- Persson, S. E., *et al.* 2004, *AJ*, 128, 2239
- Rieke, G. H., & Lebofsky, M. J. 1985, *ApJ*, 288, 618
- Riess, A. G., *et al.*, 2005, *ApJ*, 627, 579
- Román-Zúñiga, C. G., Lada, C. J., Muench, A., & Alves, J. F. 2007, *ApJ*, 664, 357
- Sandage, A. R., Tammann, G. A., Saha, A., Reindl, B., Macchetto, F. D., & Panagia, N.



2006, ApJ, 653, 843

Schaefer, B.E. 2007, AJ, (in press) = arXiv:0709.4531

Udalski, A., Szymanski, M., Kubiak, M., Pietrzynski, G., Soszynski, I, Wozniak, P., & Zebrun, K. 1999, Acta Astronomica, 49, 201

Wisnewski, W. Z., & Johnson, H. L. 1968, Comm. Lunar Planet. Lab, No. 112

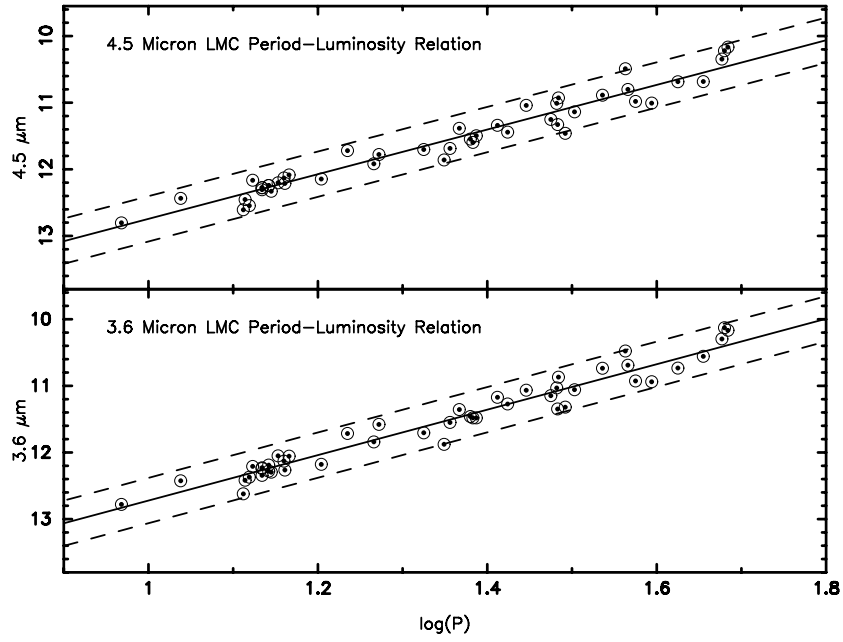


Fig. 1.— IRAC 3.6 and 4.5  $\mu\text{m}$  Period-Luminosity relations for LMC Cepheids in the  $\log(P)$  range from 0.8 to 1.8. The broken lines represent  $\pm 2\sigma$  ( $\pm 0.32$  mag) bounds on the instability strip.

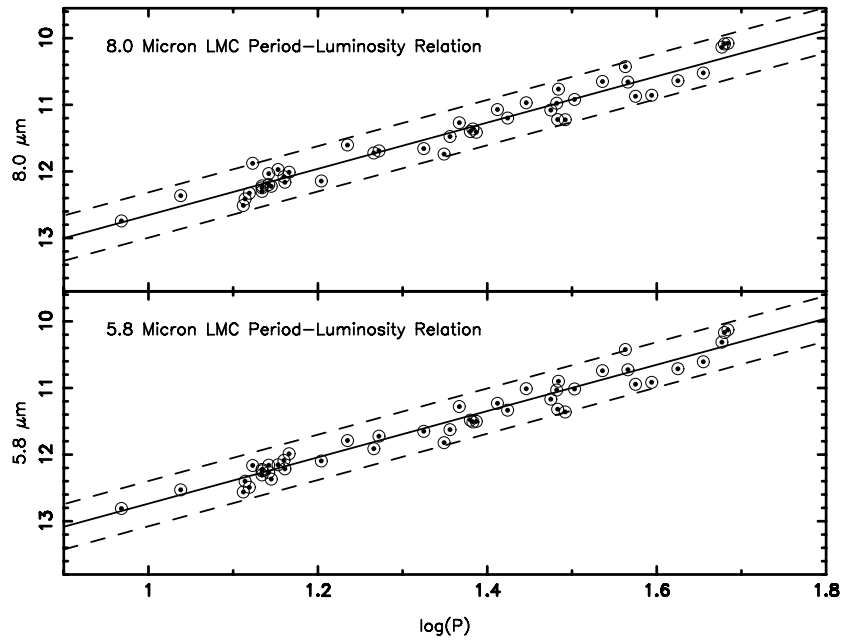


Fig. 2.— IRAC 5.8 and 8.0  $\mu\text{m}$  Period-Luminosity relations for LMC Cepheids in the  $\log(P)$  range from 0.8 to 1.8.

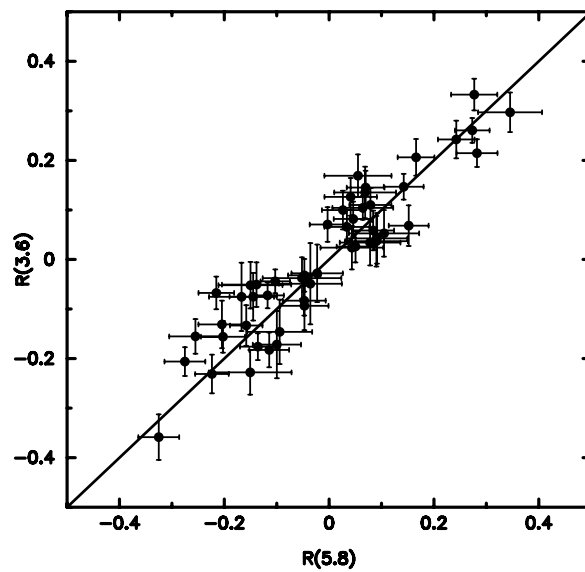


Fig. 3.— Residuals in the PL fit at 3.6  $\mu\text{m}$  versus residuals in the PL fit at 5.8  $\mu\text{m}$ , illustrating both the high degree of correlation between the residuals, accounting for most of the variance, and the small residual scatter in the correlation. The correlation is driven by the random-phase nature of the sampling of the Cepheid light curves in addition to the correlated nature of the mean properties of Cepheids within and across the instability strip. The residual noise about the mean correlation is entirely consistent with the quoted mean photometric errors in the individual data points (i.e., 0.05 mag).

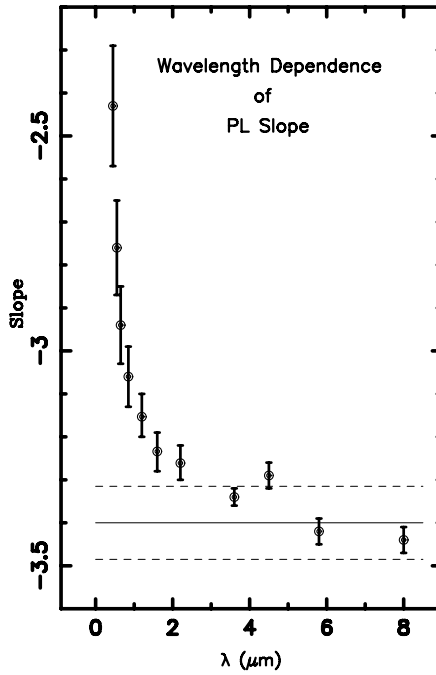


Fig. 4.— The steepening of the slope of the Cepheid Period-Luminosity relation as a function of increasing wavelength, from the optical (BVRI) through the near infrared (JHK) and out to 8 microns in the IRAC mid-infrared. An asymptotic value (predicted from the Period-Radius relation) and its one-sigma uncertainties are shown by the horizontal lines at  $-3.40 \pm 0.085$ .

,

Table 1.

Cepheid	log(P) (days)	3.6 $\mu$ m (mag)	4.5 $\mu$ m (mag)	5.8 $\mu$ m (mag)	8.0 $\mu$ m (mag)
HV 872	1.475	11.15 0.04	11.25 0.05	11.17 0.04	11.08 0.04
HV 873	1.536	10.74 0.04	10.89 0.05	10.74 0.03	10.65 0.04
HV 875	1.482	11.03 0.03	11.01 0.04	11.03 0.03	10.98 0.03
HV 876	1.356	11.55 0.04	11.69 0.05	11.63 0.05	11.48 0.05
HV 877	1.655	10.56 0.03	10.68 0.05	10.61 0.04	10.52 0.04
HV 878	1.367	11.36 0.04	11.38 0.06	11.28 0.04	11.27 0.03
HV 879	1.566	10.69 0.02	10.80 0.04	10.73 0.03	10.66 0.03
HV 882	1.503	11.06 0.03	11.14 0.05	11.02 0.04	10.92 0.03
HV 886	1.380	11.46 0.03	11.55 0.05	11.48 0.04	11.40 0.04
HV 887	1.161	12.26 0.05	12.21 0.08	12.21 0.06	12.16 0.04
HV 889	1.412	11.17 0.05	11.34 0.09	11.23 0.05	11.07 0.04
HV 891	1.235	11.72 0.05	11.72 0.06	11.79 0.05	11.60 0.04
HV 892	1.204	12.18 0.04	12.15 0.05	12.10 0.04	12.14 0.05
HV 893	1.325	11.70 0.05	11.70 0.05	11.65 0.06	11.66 0.04
HV 899	1.492	11.32 0.03	11.46 0.06	11.36 0.04	11.23 0.04

Table 1—Continued

Cepheid	log(P) (days)	3.6 $\mu$ m (mag)	4.5 $\mu$ m (mag)	5.8 $\mu$ m (mag)	8.0 $\mu$ m (mag)
HV 900	1.677	10.30	10.35	10.31	10.14
		0.03	0.04	0.03	0.03
HV 901	1.266	11.84	11.92	11.91	11.72
		0.04	0.06	0.04	0.05
HV 904	1.483	11.35	11.33	11.32	11.22
		0.03	0.03	0.03	0.03
HV 909	1.575	10.93	10.98	10.94	10.87
		0.04	0.06	0.04	0.04
HV 914	0.838	13.02	13.06	13.14	12.88
		0.04	0.08	0.05	0.07
HV 932	1.123	12.21	12.16	12.16	11.88
		0.06	0.07	0.06	0.10
HV 953	1.680	10.13	10.22	10.17	10.09
		0.03	0.05	0.04	0.03
HV 971	0.968	12.78	12.80	12.81	12.74
		0.04	0.08	0.08	0.07
HV 997	1.119	12.37	12.55	12.49	12.33
		0.04	0.06	0.06	0.05
HV 1002	1.484	10.87	10.93	10.90	10.76
		0.03	0.04	0.04	0.03
HV 1003	1.387	11.48	11.50	11.50	11.41
		0.03	0.05	0.04	0.04
HV 1005	1.272	11.58	11.78	11.72	11.69
		0.03	0.04	0.03	0.03
HV 1006	1.153	12.05	12.20	12.15	11.97
		0.05	0.06	0.06	0.04
HV 1013	1.383	11.48	11.60	11.51	11.36
		0.02	0.04	0.06	0.03
HV 1019	1.134	12.24	12.28	12.24	12.30
		0.06	0.06	0.05	0.07



Table 1—Continued

Cepheid	log(P) (days)	3.6 $\mu$ m (mag)	4.5 $\mu$ m (mag)	5.8 $\mu$ m (mag)	8.0 $\mu$ m (mag)
HV 1023	1.424	11.27	11.44	11.33	11.20
		0.04	0.04	0.03	0.03
HV 2244	1.145	12.30	12.33	12.37	12.22
		0.05	0.06	0.06	0.05
HV 2251	1.446	11.06	11.04	11.01	10.97
		0.03	0.06	0.03	0.03
HV 2257	1.594	10.94	11.01	10.91	10.86
		0.04	0.06	0.04	0.04
HV 2260	1.114	12.42	12.45	12.40	12.41
		0.04	0.05	0.04	0.04
HV 2270	1.134	12.34	12.31	12.31	12.22
		0.05	0.05	0.06	0.05
HV 2279	0.839	13.12	13.08	13.07	13.01
		0.05	0.06	0.08	0.09
HV 2282	1.166	12.06	12.08	11.99	12.01
		0.07	0.06	0.05	0.05
HV 2291	1.349	11.88	11.86	11.82	11.74
		0.04	0.07	0.06	0.04
HV 2294	1.563	10.48	10.49	10.42	10.43
		0.05	0.05	0.04	0.04
HV 2324	1.160	12.13	12.13	12.09	12.08
		0.05	0.05	0.05	0.04
HV 2337	0.837	13.14	13.19	13.25	13.15
		0.05	0.10	0.07	0.08
HV 2338	1.625	10.73	10.69	10.71	10.64
		0.03	0.05	0.04	0.03
HV 2339	1.142	12.28	12.24	12.27	12.20
		0.04	0.05	0.06	0.05
HV 2352	1.134	12.23	12.27	12.22	12.24
		0.08	0.05	0.06	0.07

Table 1—Continued

Cepheid	log(P) (days)	3.6 $\mu$ m (mag)	4.5 $\mu$ m (mag)	5.8 $\mu$ m (mag)	8.0 $\mu$ m (mag)
HV 2369	1.684	10.17	10.17	10.13	10.08
		0.04	0.05	0.03	0.04
HV 2405	0.840	13.37	13.33	13.35	13.32
		0.05	0.05	0.07	0.08
HV 2432	1.038	12.43	12.44	12.53	12.36
		0.07	0.05	0.06	0.05
HV 2527	1.112	12.62	12.61	12.56	12.51
		0.03	0.06	0.04	0.06
HV 2538	1.142	12.19	12.24	12.16	12.03
		0.03	0.03	0.04	0.03
HV 2549	1.209	11.71	11.76	11.74	11.67
		0.04	0.06	0.05	0.04
HV 2579	1.128	12.08	12.12	12.08	12.02
		0.04	0.05	0.05	0.06
HV 2580	1.228	11.69	11.82	11.76	11.66
		0.03	0.03	0.03	0.03
HV 2733	0.941	12.86	12.82	12.85	12.76
		0.05	0.05	0.05	0.07
HV 2749	1.364	11.69	11.77	11.69	11.49
		0.04	0.06	0.05	0.05
HV 2793	1.283	11.50	11.62	11.56	11.47
		0.03	0.06	0.05	0.04
HV 2836	1.244	11.93	12.03	11.91	12.01
		0.03	0.05	0.05	0.04
HV 2854	0.936	12.91	12.88	12.94	12.83
		0.03	0.04	0.04	0.05
HV 5655	1.153	12.14	12.18	12.11	12.06
		0.05	0.06	0.05	0.05
HV 6065	0.835	13.17	13.26	13.16	13.28
		0.04	0.06	0.07	0.08

Table 1—Continued

Cepheid	log(P) (days)	3.6 $\mu$ m (mag)	4.5 $\mu$ m (mag)	5.8 $\mu$ m (mag)	8.0 $\mu$ m (mag)
HV 6098	1.384	11.14 0.03	11.13 0.04	11.14 0.03	11.10 0.02
HV 8036	1.453	11.19 0.04	11.31 0.06	11.22 0.04	11.24 0.04
HV 12471	1.200	12.00 0.04	12.13 0.05	12.03 0.05	11.96 0.05
HV 12505	1.158	12.39 0.04	12.45 0.05	12.53 0.08	12.41 0.05
HV 12656	1.127	12.31 0.05	12.30 0.05	12.29 0.05	12.25 0.05
HV 12700	0.911	12.88 0.04	12.90 0.06	12.99 0.07	12.85 0.06
HV 12724	1.138	12.29 0.05	12.36 0.05	12.34 0.06	12.27 0.05
HV 12815	1.416	11.03 0.04	11.12 0.05	11.06 0.04	10.96 0.03
HV 12816	0.973	12.87 0.05	12.84 0.05	12.90 0.07	12.91 0.06
HV 13048	0.836	13.06 0.03	13.09 0.05	13.07 0.05	13.00 0.06